Numerical Solution of 2-D Scattering Problems Using High-Order Methods

Lisa R. Hamilton, John J. Ottusch, Mark A. Stalzer, R. Steven Turley, *Senior Member, IEEE*, John L. Visher, and Stephen M. Wandzura

***Abstract*—We demonstrate that a method of moments scattering code employing high-order methods can compute accurate values for the scattering cross section of a smooth body more efficiently than a scattering code employing standard low-order methods. Use of a high-order code also makes it practical to provide meaningful accuracy estimates for computed solutions.**

***Index Terms*— Boundary integral equation, electromagnetic scattering, high-order numerical method, method of moments.**

I. Introduction

A common misconception about method of moments solutions to scattering problems is that they cannot produce results accurate to more than a few decimal places. Such a limitation cannot be fundamental. The method of moments technique results from discretizing an integral formulation of the wave equation, which, in its continuous form, is exact. We expect that the solution to the discretized integral equation will converge to the solution of the continuous integral equation in the limit as the discretization scale size is reduced to zero, if finite precision effects are negligible.

The problem with achieving high accuracy is not a fundamental one but rather a practical one, and it stems from the almost universal use of low-order numerical methods in scattering codes. Low-order numerical methods, while simpler to implement, suffer from the fact that the computer resources (e.g., memory and CPU time) required to achieve a given solution accuracy grow rapidly as the accuracy requirement increases. Even for scatterers only a few wavelengths in size, the computer resources required to compute cross sections to more than a few digits of accuracy may be excessive. High-order methods are specifically designed to overcome such limitations by reducing the incremental cost of accuracy improvements.

FastScat™ is a general purpose, method of moments scattering code [1] developed at Hughes Research Laboratories (now HRL Laboratories) that employs high-order methods in its current basis functions, quadratures, and geometry description. The focus of this paper is on the current basis functions and how they influence the convergence rate of computed cross sections for two dimensional (2-D) scattering problems. We will demonstrate that high-order methods make it practical to achieve solution accuracies limited only by machine precision. Such a demonstration is not merely of academic interest. High accuracies at intermediate stages of the calculation are sometimes required to achieve even engineering accuracies in the final result. Furthermore, the ability to obtain accuracy improvements at relatively low cost has the added benefit that it becomes possible to obtain meaningful estimates of the accuracy of a computed solution [2]. Without some estimate of its accuracy, a computed solution is of limited usefulness.

Manuscript received September 22, 1997; revised July 24, 1998. This work was supported by the Advanced Research Projects Agency of the U.S. Department of Defense and was monitored by the Air Force Office of Scientific Research under Contracts F49620-91-C-0064 and F49620-91-C-0084.

L. R. Hamilton, J. J. Ottusch, M. A. Stalzer, J. L. Visher, and S. M. Wandzura are with the Computational Physics Department of the Information Sciences Laboratory at HRL Laboratories, Malibu, CA 90265 USA.

R. S. Turley is with the Department of Physics and Astronomy at Brigham Young University, Provo, UT 84602 USA.

Publisher Item Identifier S 0018-926X(99)04775-4.

II. Scalar Integral Equations

The electromagnetic scattering problem for a three-dimensional (3-D) scatterer that is translationally invariant in one direction can be decoupled into two independent problems, each of which is isomorphic to a two dimensional scalar scattering problem with a different boundary condition. In the TM case, the incident electric field is polarized parallel to the axis of symmetry; in the TE case, it is the incident magnetic field. The boundary conditions for the 2-D scalar scattering problem corresponding to a perfect electrical conductor (PEC) in 3-D are Dirichlet for TM polarization and Neumann for TE polarization.

For the TM polarization case [$\psi(\boldsymbol{x}'$ on $C) = 0$], the electric field integral equation for PEC boundary conditions is

$$\phi^{\text{inc}}(\boldsymbol{x}) = -\oint_C dl'\, G(\boldsymbol{x}, \boldsymbol{x}')\sigma(\boldsymbol{x}') \tag{1}$$

where ϕ^{inc} is the incident field and σ is the surface charge density. It is defined as the normal derivative of the total field ψ on the surface, i.e.,

$$\sigma(\boldsymbol{x}') \equiv -\hat{\boldsymbol{n}}' \cdot \boldsymbol{\nabla}\psi(\boldsymbol{x}') \tag{2}$$

where $\hat{\boldsymbol{n}}'$ is the outward normal to the scattering surface at $\boldsymbol{x}'$. The integral is taken around the contour C given by the intersection of the 3-D scattering surface and a plane perpendicular to the axis of symmetry. The kernel G is the Green function of the Helmholtz wave equation in 2-D, namely

$$G(\boldsymbol{x}, \boldsymbol{x}') = \frac{i}{4} H_0^{(1)}(k|\boldsymbol{x} - \boldsymbol{x}'|) \tag{3}$$

where $H_0^{(1)}$ is the zeroth-order Hankel function of the first kind and k is the wavenumber of the incident field. Similarly, for the TE polarization case [$\sigma(\boldsymbol{x}'$ on $C) = 0$], the electric field integral equation is

$$-\hat{\boldsymbol{n}} \cdot \boldsymbol{\nabla}\phi^{\text{inc}}(\boldsymbol{x}) = (\hat{\boldsymbol{n}} \cdot \boldsymbol{\nabla}) \oint_C dl'(\hat{\boldsymbol{n}}' \cdot \boldsymbol{\nabla}' G(\boldsymbol{x}, \boldsymbol{x}'))\psi(\boldsymbol{x}'). \quad (4)$$

The correspondence between the scalar quantities ψ and σ and the parallel (to the surface) components of the electric and magnetic fields is given by

$$\boldsymbol{E}_{||}(\boldsymbol{x}) = \psi(\boldsymbol{x})\hat{\boldsymbol{z}} \quad (5)$$

$$\boldsymbol{H}_{||}(\boldsymbol{x}) = \frac{\sigma(\boldsymbol{x})}{i\omega\mu}\hat{\boldsymbol{z}} \times \hat{\boldsymbol{n}} \quad (6)$$

in the TM case and

$$\boldsymbol{H}_{||}(\boldsymbol{x}) = \psi(\boldsymbol{x})\hat{\boldsymbol{z}} \quad (7)$$

$$\boldsymbol{E}_{||}(\boldsymbol{x}) = \frac{\sigma(\boldsymbol{x})}{i\omega\epsilon}\hat{\boldsymbol{n}} \times \hat{\boldsymbol{z}} \quad (8)$$

in the TE case, where $\hat{\boldsymbol{z}}$ is the direction of translational invariance, $\hat{\boldsymbol{n}}$ is the surface normal, ω is the angular frequency, and ϵ and μ are the dielectric constant and magnetic susceptibility of the external medium, respectively. All fields implicitly contain the time dependence factor $e^{i\omega t}$.

A Galerkin method of moments solution [3] to the continuous scalar field equation, (1), proceeds by first expanding the unknown charge $\sigma(\boldsymbol{x})$ in terms of basis functions $f_j(\boldsymbol{x})$,

$$\sigma(\boldsymbol{x}) = \sum_j I_j f_j(\boldsymbol{x}) \quad (9)$$

and then testing the equation with each of the basis functions by applying the operator $\oint_C ds'\ f_i(\boldsymbol{x}')\cdot$ to both sides. The result is a matrix equation of the form

$$V = ZI \quad (10)$$

where

$$V_i = \oint_C dl\ \phi^{\text{inc}}(\boldsymbol{x}) f_i(\boldsymbol{x}) \quad (11)$$

and

$$Z_{ij} = \oint_C dl \oint_C dl'\ f_i(\boldsymbol{x}) G(\boldsymbol{x}, \boldsymbol{x}') f_j(\boldsymbol{x}'). \quad (12)$$

Similarly, we can discretize the scalar charge equation, (4), by expanding the unknown field as

$$\psi(\boldsymbol{x}) = \sum_j S_j f_j(\boldsymbol{x}) \quad (13)$$

and applying the testing operators to arrive at the matrix equation

$$\tilde{V} = \tilde{Z}S \quad (14)$$

where

$$\tilde{V}_i = -\oint_C dl\ [\hat{\boldsymbol{n}} \cdot \boldsymbol{\nabla}\phi^{\text{inc}}(\boldsymbol{x})] f_i(\boldsymbol{x}) \quad (15)$$

and

$$\tilde{Z}_{ij} = \oint_C dl\ f_i(\boldsymbol{x})(\hat{\boldsymbol{n}} \cdot \boldsymbol{\nabla}) \oint_C dl'(\hat{\boldsymbol{n}}' \cdot \boldsymbol{\nabla}' G(\boldsymbol{x}, \boldsymbol{x}'))f_j(\boldsymbol{x}') \quad (16a)$$

$$= \oint_C dl \oint_C dl'\ f_i(\boldsymbol{x}) \cdot \left[\left(k^2(\hat{\boldsymbol{n}} \cdot \hat{\boldsymbol{n}}') - \frac{\partial^2}{\partial l \partial l'}\right) G(\boldsymbol{x}, \boldsymbol{x}')\right] f_j(\boldsymbol{x}') \quad (16b)$$

$$= \oint_C dl \oint_C dl' \cdot \left[k^2(\hat{\boldsymbol{n}} \cdot \hat{\boldsymbol{n}}') f_i(\boldsymbol{x}) f_j(\boldsymbol{x}') - \frac{\partial f_i(\boldsymbol{x})}{\partial l}\ \frac{\partial f_j(\boldsymbol{x}')}{\partial l'}\right] G(\boldsymbol{x}, \boldsymbol{x}'). \quad (16c)$$

The second form for $\tilde{Z}_{ij}$ is like the first in that it requires differentiating the kernel twice. In the first form they are normal derivatives; in the second they have been converted to tangential derivatives by use of the Helmholtz equation. Differentiating the kernel exacerbates the singularity of the kernel at $\boldsymbol{x} = \boldsymbol{x}'$, which is unattractive from a numerical standpoint unless some smoothing operator is applied to the kernel before differentiation. FastScat uses a high-order regulated kernel [4] that is analytic everywhere to avoid this difficulty. The third form is obtained from the second by twice integrating by parts. This reduces the singularity of the kernel to that of the Dirichlet case. It does, however, require basis functions that are differentiable.

III. High-Order Methods

FastScat uses patch-based basis functions for both the TM and TE polarization cases. That is to say the basis functions are nonzero only on individual patches. The patches are arbitrarily curved line segments parameterized by a function $\boldsymbol{x}(u), 0 \le u \le 1$. The basis functions are defined in terms of the surface parameterization according to

$$f_n(u) = \frac{\sqrt{2n+1}}{4\sqrt{g(u)}} P_n(2u-1) \quad (17)$$

where P_n is the nth Legendre polynomial and

$$g(u) = \left(\frac{\partial x}{\partial u}\right)^2 + \left(\frac{\partial y}{\partial u}\right)^2 \quad (18)$$

is the metric for the patch [5]. The normalization factors are chosen to make the basis functions orthonormal when integrated over a patch, i.e.,

$$\int_{\text{patch}} dl\ f_m(\boldsymbol{x}) f_n(\boldsymbol{x}) = \int_0^1 du\ \sqrt{g(u)} f_m(u) f_n(u) = \delta_{mn}. \quad (19)$$

The contribution to the overall solution error due to surface misrepresentation can be eliminated by internally representing the surface using its exact functional form [6]. Using the combination of high-order basis functions and an exact surface representation, FastScat can obtain a high-order approximation

to the smoothly varying source distribution that is to be expected on a smooth scattering surface.

By contrast, standard, low-order method of moments implementations use flat segments to approximate the surface geometry and basis functions that are constant (in the TM case) or piecewise linear (in the TE case) on a patch to approximate the sources. Representing a smoothly curved scatterer using flat segments is an example of surface representation error. Using flat segments further degrades the accuracy of the computation by introducing artificial edges, which cause spurious diffraction. Constant (or "pulse") basis functions are equivalent to the zeroth-order basis functions in FastScat; piecewise linear (or "rooftop") basis functions can be constructed from FastScat's zeroth-order and first-order basis functions. The advantage of having higher order polynomial basis functions is that they can provide accurate approximations to smooth functions more efficiently than pulse or rooftop basis functions alone can.

The third numerical method that must be high order to achieve high-order convergence in the final result involves numerical evaluation of integrals such as those in (12) and (16). Gaussian quadrature is a well-known high-order method for evaluating integrals of nonsingular integrands. The impedance matrix elements of (12) and (16) fall into this category when the regions of integration of $\boldsymbol{x}$ and $\boldsymbol{x}'$ do not intersect. Such integrals may be evaluated efficiently with Gaussian quadrature and typically are, even in standard method of moments codes. The trouble begins when the regions of integration *do* intersect, as occurs when the patches involved touch or are the same. In such cases, standard Gaussian quadrature is reduced to the status of a low-order method [7], [8]. So-called "singularity removal" (which is misnamed because, although it removes the infinity in the kernel at $\boldsymbol{x} = \boldsymbol{x}'$, it does not eliminate the singularity of the kernel at $\boldsymbol{x} = \boldsymbol{x}'$ in the strict mathematical sense) is often called upon to handle such integrals, even though it does not actually restore the high-order behavior of Gaussian quadrature.

Several schemes for high-order evaluation of singular integrands have been devised for and implemented in FastScat. One involves using quadrature rules that are specific to the singularity. For 2-D, where the singularity of the kernel is logarithmic, high-order "lin-log" rules [9] have been developed. They are designed to exactly integrate products of polynomials and logarithms. An alternate approach that is more easily extended to the 3-D scattering case, involves tampering with the kernel to eliminate the singularity at $\boldsymbol{x} = \boldsymbol{x}'$, but doing it in such a way that convolutions of the kernel with polynomial functions are still computed exactly [4]. The resulting function is regular (i.e., analytic)—hence, the name "regulated kernel". Convolutions of smooth functions with an appropriate regulated kernel may be evaluated in a high-order fashion by means of standard Gaussian quadrature. Both of these methods lead to similar results. The calculations reported in this paper were performed using a high-order regulated kernel and Gaussian quadrature.

High-order methods have the potential to greatly improve the efficiency of obtaining accurate numerical results. However, like a chain whose strength is limited by its weakest link, the convergence rate of an algorithm whose final result depends on several numerical methods, is limited by the convergence rate of its lowest order method. For scattering computations, this applies to the numerical methods used for surface representation, basis functions, and quadratures. To show how the method order of one of these components affects the rate of convergence of the full solution, it is best to vary that one while setting the method order for each of the other two components high enough that they do not contribute any noticeable error. With FastScat, the user can control the order of each of these three numerical methods.

The focus of this paper is on high-order basis functions and how they can be employed to efficiently compute accurate results. Therefore, the calculations summarized here show the effect of varying the basis function order while using exact surface representations and quadrature orders high enough that numerical integration error was negligible. In normal usage, one generally uses exact surfaces and sets the orders of the basis functions and the quadratures to be no higher than necessary to achieve the desired accuracy in the final result.

IV. Results

Measuring the order of convergence of a numerical method requires observing how the error in the final result responds to changes in the discretization. For small enough discretization scales h, we expect the error to scale as $\epsilon \sim h^n$ for an nth-order numerical method.

In this next two sections, we present results of FastScat calculations on canonical 2-D geometries (a circle and an ellipse) that demonstrate how the rate of convergence varies with discretization scale size and basis function order. The third subsection is devoted to a large 2-D scattering geometry we call the "bat." The bat is prototypical of scatterers whose cross section has a large dynamic range as a function of angle. For such scatterers, the utility of a high-order scattering code becomes evident even at "practical" accuracies. Sun SPARC 10's were used for the circle calculations; the ellipse and bat calculations were performed on IBM RS/6000 computers.

A. Circle

The circle is one of the best geometries to use for investigating the convergence properties of a scattering code because it has no geometrical singularities (e.g., edges and corners) and the answer can be computed to arbitrary accuracy by summing the Mie series. This means that we can determine exactly and unambiguously what the errors are in our computed solutions, which eliminates one of the sources of disagreement about how to quantify solution accuracy.

We used FastScat to compute the bistatic cross section of 1λ-radius circles for Dirichlet and Neumann boundary conditions, corresponding to TM and TE polarizations, respectively. The circles were divided into equal segments, each segment being represented internally as a circular arc. Quadrature orders were set high enough to guarantee that numerical integrations would be accurate to better than one part in 10^{12}.

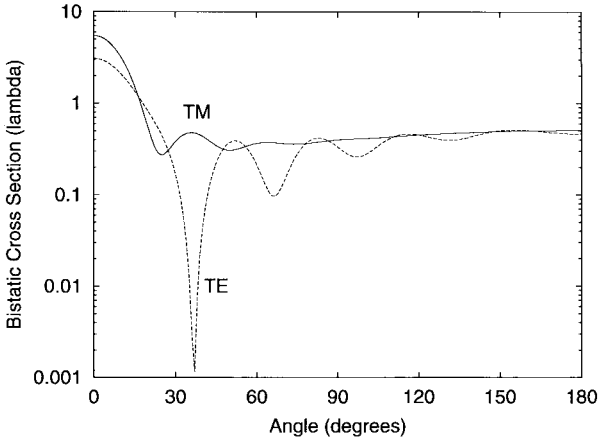

Fig. 1. Bistatic cross section of a 1λ-radius circle for TM and TE polarization (Mie series).

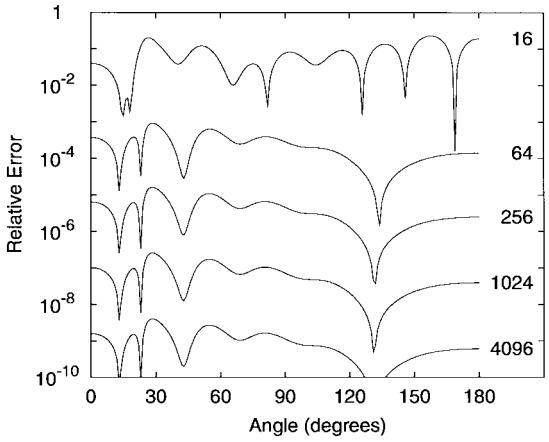

Fig. 2. Fractional difference between the cross section computed by FastScat using pulse basis functions and the exact cross section (Fig. 1) as a function of observation angle. The curves are labeled by the number of identical segments into which the 1λ-radius circle was divided.

We performed a series of calculations with different basis function orders and different numbers of segments, and compared against the exact results (Fig. 1). A sample of the results is shown in Fig. 2 for the case of zeroth-order basis functions and TM polarization. The error in the cross section varies as a function of bistatic scattering angle. It is evident, however, that, for 64 or more patches, increasing the number of patches by a factor of four reduces the overall error by a factor of about 64.

We can make a stronger quantitative statement about the discretization error if we condense the error versus angle information into a single number for each discretization. Of the many ways to do this, we have investigated three: maximum relative error, maximum error ÷ average cross section, and root mean square (rms) error. For this particular problem, the result is essentially independent of which measure of error is chosen. Fig. 3 shows maximum relative error $(\max[|\mathrm{RCS}(\theta)/\mathrm{RCS}_{\mathrm{ref}}(\theta) - 1|])$ versus density of unknowns plotted on a log–log scale for basis function orders zero, one, and two, and numbers of patches ranging from four to 4096. Consider the TM polarization case first. The most important feature to note is that, for enough unknowns, the data fit a

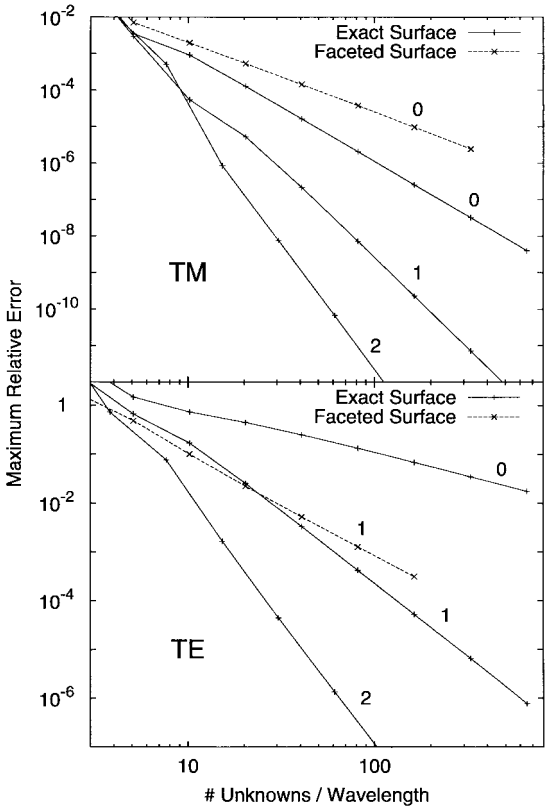

Fig. 3. Log-log plot of maximum relative error versus density of unknowns for the TM and TE polarization cases. Each set of points is labeled by basis function order.

linear trend line whose slope increases as the basis function order increases. Since the discretization scale h is inversely proportional to the number of unknowns N, this simply reflects the fact that the error diminishes as h^m, where m increases with method order. In fact, the slopes of the lines connecting constant basis function points are close to integers—three for zeroth-order, five for first-order, and seven for second-order—indicating that the order of convergence of the cross section when using nth-order basis functions is $m = 2n + 3$.

On the same plot, we also show an example of how the surface model affects the convergence rate. The dashed curve connects points that were computed by replacing the circular arc patches with flat patches. The order of the quadratures was the same as in the previous case. For this case, however, only one basis function order is shown, namely zero. The reason is that the poor surface representation so limits the rate of convergence that increasing the order of the basis functions has essentially no effect on the accuracy of the solution. Curves for higher basis function orders are virtual copies of the zeroth-order result, shifted to higher numbers of unknowns. In all such cases, the error in the cross section is consistent with h^2 scaling.

In the TE case, the slopes of the lines connecting constant basis function points are close to one for zeroth order, three for first order, and five for second order, indicating that the order of convergence of the cross section when using nth-order basis functions is $x = 2n + 1$. The dashed curve connects points computed according to the standard method

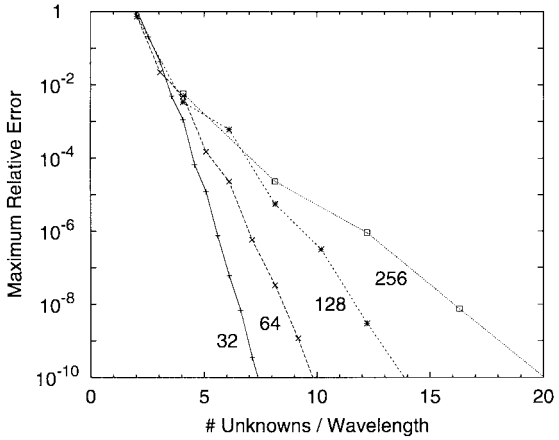

Fig. 4. Semilog plot of maximum relative error versus density of unknowns for TM scattering from a 10λ-radius circle. Points corresponding to different basis function orders for a fixed patch size are connected by lines and labeled by the number of patches.

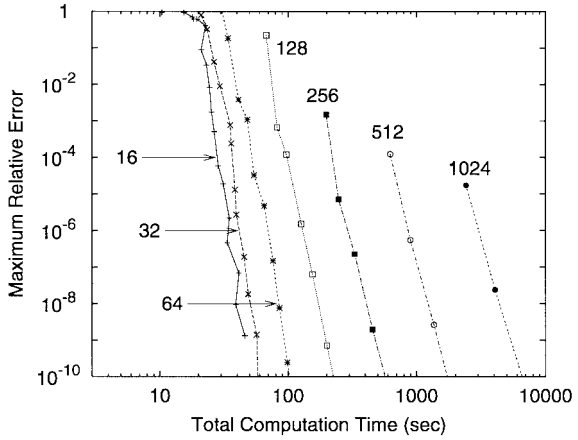

Fig. 5. Log-log plot of maximum relative error versus total computation time required to calculate the bistatic cross section of a 10λ-radius circle with TM polarization. Points corresponding to different basis function orders and a fixed patching are connected by lines, which are labeled by the number of equal arc length patches used.

of moments procedure for TE polarization, namely, by putting rooftop basis functions on a faceted approximation to the scatterer. It converges more rapidly than do the calculations that used zeroth-order (i.e., pulse) basis functions with an exact geometry representation. This is not surprising given that currents modeled by rooftop basis functions are guaranteed to be continuous across patch boundaries, whereas those modeled by pulse basis functions are not. As in the TM case, however, using higher order basis functions, whether patch-based or edge-based, does not improve the order of convergence when a low-order geometry representation is used. It only increases the number of unknowns used to achieve a given accuracy. In all such cases, the error in the cross section is consistent with h^2 scaling.

Since memory usage is proportional to N^2, these plots also show how method order affects the relationship between accuracy and memory used. For errors less than about 10^{-4} in the TM case and one in the TE case, not only are the errors in the cross sections lower when high-order methods are employed, but also the marginal cost of additional accuracy is lower.

In the plots shown so far, curves connect data points corresponding to decreasing patch sizes at a constant method order. In finite element terminology this is known as "h-refinement." As we have seen, h-refinement on a smooth scatterer results in geometric convergence in the cross section. Alternatively, one can take the same data and make a plot by connecting points of increasing method order for a fixed patch size. This is known as "p-refinement." The result of doing this for bistatic scattering from a 10λ-radius circle and TM polarization is shown in Fig. 4. The curves tend toward straight lines, which, on a semilog plot, indicates exponential convergence. Exponential convergence in the computed cross section is characteristic of p-refinement on a smooth scatterer when high-order polynomial basis functions are used.

Methods that achieve high-order convergence in general, and exponential convergence in particular, have obvious advantages for efficiently computing accurate cross sections. What may be less obvious is the fact that they facilitate accuracy estimation for computed solutions. For example, suppose we had not had an independent means (such as the Mie series for a circle) for computing a suitably accurate reference solution. We could still obtain an estimate of the accuracy of a given computed solution by comparing it to a reference solution generated by redoing the computation with an even finer discretization. To be useful, however, the reference solution must be significantly more accurate than the comparison solution. Obtaining a suitable reference solution using low-order methods may require doubling or quadrupling the number of patches, and hence the number of unknowns. The additional cost of such a calculation may be so high as to make it impractical. On the other hand, generating the reference solution by increasing the basis function order can produce a significantly better answer with only a modest increase in the number of unknowns. The increase in required memory and computation time is likewise modest. In our opinion, the widespread reliance on low order methods is what accounts for the fact that it is virtually unheard of to see accuracy estimates accompanying computed cross sections.

Another observation that may be made from Fig. 4 is that the way to achieve a high accuracy result using the least memory (i.e., fewest unknowns) is to make the patches large and put high-order basis functions on them. A look at run times instead of unknowns/memory usage leads to the same conclusion. Fig. 5 shows that for TM scattering from a 10λ-radius circle, the total computation time required to achieve a given accuracy decreases as the number of patches decreases. A point of diminishing returns is reached at around 16 patches, at which point the arc length of each patch is about 4λ. The optimum distribution of patch sizes for an arbitrary scatterer will depend on its geometry. The general rule of thumb that we follow for patching smooth scatterers is to make the patches about one wavelength long, except in regions where the geometry is strongly curved. In such regions, the patches should be some moderate fraction of the local radius of curvature.

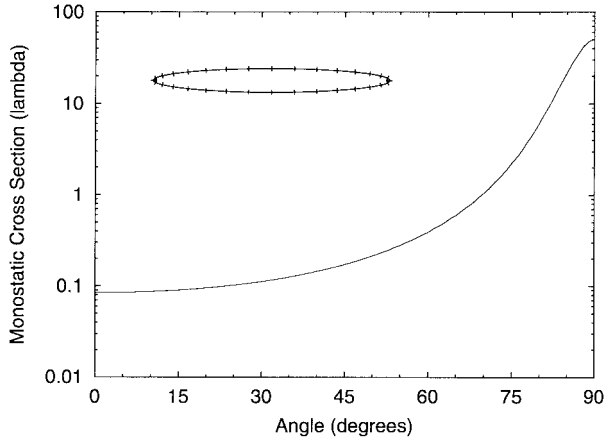

Fig. 6. Monostatic cross section of a $20\lambda \times 2\lambda$ ellipse (shown with 32 patches) for TM polarization.

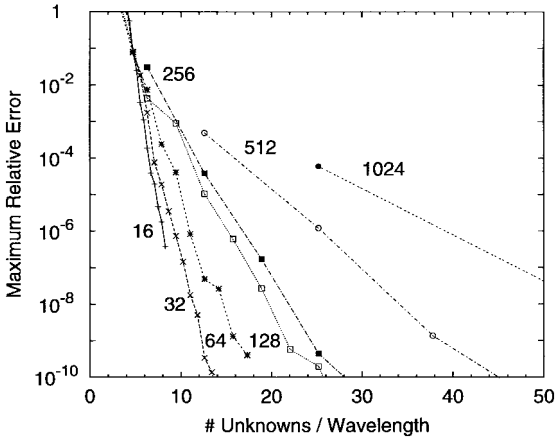

Fig. 7. Semilog plot of maximum relative error versus density of unknowns for TM scattering from a $20\lambda \times 2\lambda$ ellipse. Points corresponding to different basis function orders for a fixed patch size are connected by lines and labeled by the number of patches.

B. Ellipse

A good candidate geometry on which to apply this rule of thumb is the $20\lambda \times 2\lambda$ ellipse. We can describe the ellipse by the parametric equations

$$x = a\cos u \tag{20a}$$

$$y = b\sin u \tag{20b}$$

where $a = 10\lambda$ and $b = 1\lambda$. A sensible patching, which puts the highest density of patches in the most highly curved regions and vice versa for the flatter regions, is obtained if the patches cover equal increments in the parameter u, as indicated in the inset to Fig. 6.

We used FastScat to compute the monostatic cross section in TM polarization of a $20\lambda \times 2\lambda$ ellipse using several different combinations of basis function order and number of patches. In all cases, an exact surface representation was used to eliminate surface representation error, and the quadrature order was set high enough to guarantee that quadrature error would have an insignificant effect on the final accuracy. The reference solution was computed by putting tenth-order basis functions on an ellipse divided into 160 patches. Although we did not know the accuracy of the reference solution *a priori*, we have deduced from the convergence behavior of the comparison solutions that it is at least ten digits. A plot of the monostatic cross section versus angle for the reference solution is given in Fig. 6.

Fig. 7 demonstrates that one can realize exponential convergence in the cross section by using high-order basis functions with a fixed patching. In the high-accuracy regime, memory usage is optimized by using large patches and high-order basis functions. In the low-accuracy regime, the accuracy is not that sensitive to the discretization for a given density of unknowns. The accuracy at which the various curves tend to bunch up is geometry dependent, but, as a general rule, can be expected to decrease as the problem size increases.

The analog to Fig. 5 for the ellipse is Fig. 8.

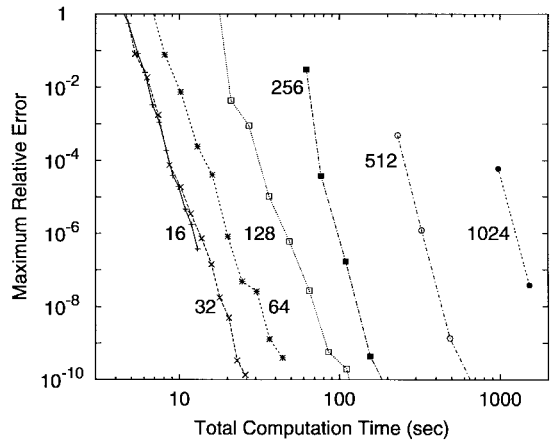

Fig. 8. Log-log plot of maximum relative error versus total computation time required to calculate the monostatic cross section of a $20\lambda \times 2\lambda$ ellipse with TM polarization. Points corresponding to different basis function orders and a fixed patching are connected by lines, which are labeled by the number of patches used.

C. 300λ Bat

A bat is composed of straight faces connected smoothly by circular arcs of radius R. There are two long edges of length L

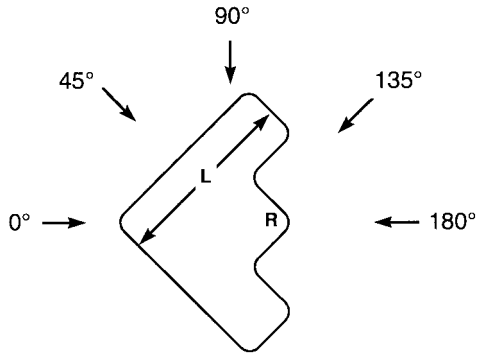

Fig. 9. "Bat" geometry.

and six short edges, each of length $L/3$, at right angles to each other. The surfaces of the corresponding 3-D bat are assumed to be perfect conductors. It is interesting from a practical point of view because it has three high cross section specular reflection regions (one of which is the 2-D analog of a corner cube) and a low cross section everywhere else (see Fig. 9).

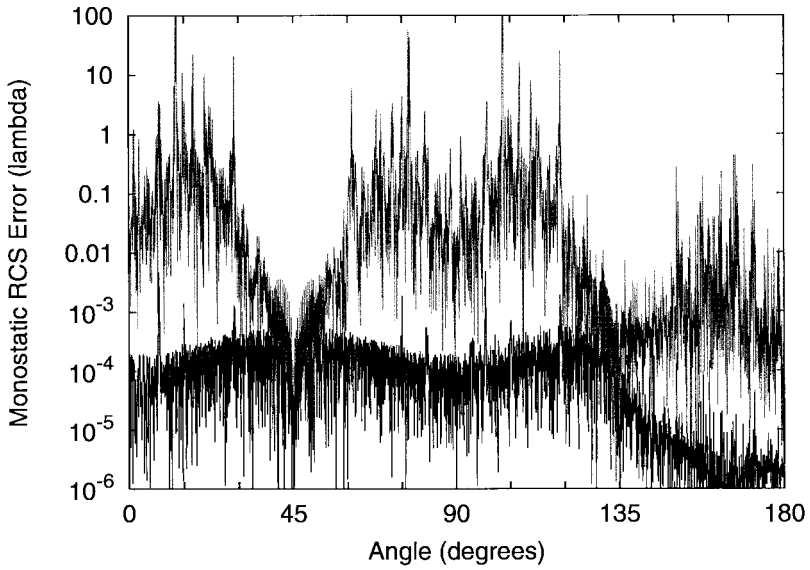

Fig. 10. Monostatic RCS of $R = 1\lambda, L = 300\lambda$ bat in TM polarization. Low-order result computed using zeroth-order basis functions on $\frac{1}{5}\lambda$ patches. High-order result computed using fourth-order basis functions on 1λ patches. Both computations used 6000 unknowns.

The results shown here are for $R = 1\lambda, L = 300\lambda$. Fig. 10 shows two computations of the monostatic cross section as a function of incidence angle for Dirichlet boundary conditions (i.e., TM polarization). One computation was performed using low-order basis functions, the other used high-order basis functions. Both calculations used an exact surface representation, quadratures good to at least eight digits of accuracy, and exactly 6000 unknowns to represent the sources. In the former case, the surface was broken up into 6000 segments, each about $\frac{1}{5}\lambda$ long, and the sources were represented by pulse basis functions (i.e., one unknown per segment). This constitutes the standard, low-order procedure (except for the exact surface representation used on the circular arcs) for solving a 2-D scattering problem with TM polarization. In the latter case, the surface was divided into 1200 patches, each about 1λ long, and basis functions up to fourth-order were employed to represent the sources (i.e., five unknowns per segment).

The two plots are very similar over a good portion of the angular range, particularly in regions of high cross section. There are narrow peaks at 45 and 135° as expected and a broader peak centered at 180°, resulting from the "corner square" effect. Note that the oscillations evident in the cross section are the result of interference, not due to any solution error. However, in the angular ranges from 0 to 30° and 60 to 120°, there are significant disagreements. The "spikes" in the upper plot Fig. 10 are suspicious looking. Which is right? How can one be sure?

Having high-order methods at one's disposal makes it possible to answer these questions with the kind of certainty that is impractical to attain with low-order methods. If we keep the same patching of the bat, but allow up to fifth-order basis functions instead, the number of unknowns increases to 7200. This corresponds to a 44% increase in the amount of memory required to store the impedance matrix and a 73% increase in the amount of CPU time required to LU decompose the impedance matrix (which is the most time-consuming step in the solution process). More importantly, allowing for one higher polynomial order to represent the sources improves the accuracy of the solution significantly. So much so that we are justified in using the fifth-order solution as a reference solution against which we can compare the lower-order solutions in order to estimate their accuracies. To compute a reference solution of comparable accuracy by the standard, low-order technique would require subdividing the 6000 patches many times into smaller patches. The number of unknowns would increase significantly. In principle, it could be done, but since CPU time for LU decomposition and memory for impedance matrix storage scale so badly with number of unknowns, the cost would be so exorbitant as to make the procedure impractical.

Fig. 11 shows plots of the differences between the fifth-order reference solution and the two solutions plotted in Fig. 10. It is evident that the fourth-order solution is the better of the two. As expected, the error is least where the cross section is highest. The estimated error of the fourth-order solution is generally below $10^{-3}\lambda$; at a few angles it rises to almost $10^{-2}\lambda$. If error bars were to be plotted on the high-order data of Fig. 10, they would all be less than the thickness of the plotted line. Fig. 11 also shows the estimated error of the low-order solution to be generally higher. Whereas it is probably acceptable over angular regions where the cross section is high, in the low cross section region the error cannot be considered acceptable, exceeding, as it does, 20 dB for certain angles. Similar results obtain for TE polarization.

V. Summary

The unfavorable tradeoff between cost and problem size for method of moments solutions to scattering problems is well known and several so-called "fast" methods, such as the fast

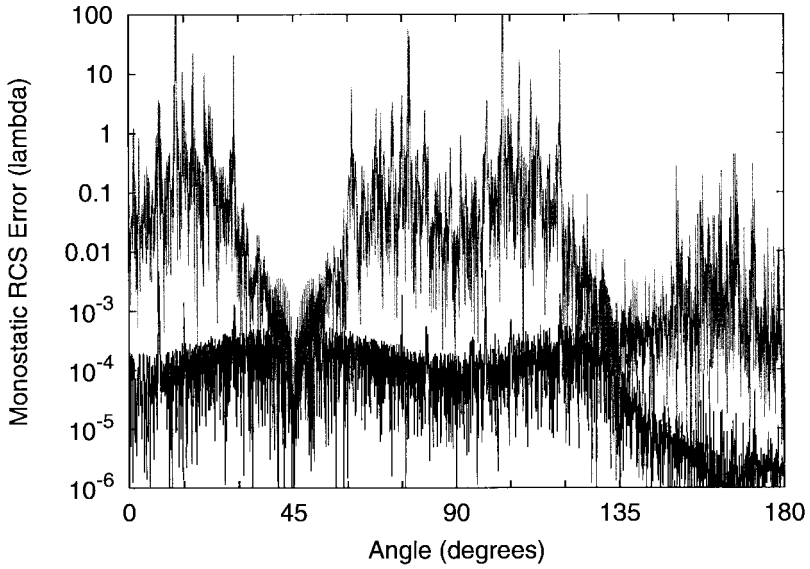

Fig. 11. RCS error with respect to reference solution computed with fifth-order basis functions on 1λ patches (7200 unknowns). Upper curve: zeroth-order calculation; lower curve: fourth-order calculation.

multipole method [10], have been devised in recent years to address it.

The subject of this paper is another tradeoff that, while no less important, is apparently much less widely appreciated. It is the tradeoff between cost and accuracy for a fixed problem size. Improving the accuracy of a computed solution requires refining the discretization, which in turn requires more memory and more computation time. With low-order methods the amount of additional computer memory and time required to achieve a more accurate result may be substantial. High-order methods are designed to make accuracy improvements much less costly.

The focus in this paper has been on using high-order basis functions to compute cross sections in 2-D. High-order basis functions are part of the triad of high-order methods that make FastScat a high-order scattering code. The results show that by using high-order methods it is possible to achieve very accurate solutions to simple scattering problems on a workstation in a reasonable amount of time. Furthermore, we have demonstrated that the solution converges at a geometric rate as a function of patch size for fixed basis function order and exponentially as a function of basis function order for fixed patch size. For high accuracies, the most computationally efficient solutions, in terms of both memory and CPU time, are produced by using high-order basis functions on large patches.

High-order methods are important for doing large problems as well. In fact, the adverse effects of a low-order discretization are likely to manifest themselves even more prominently as problems grow in size. The error caused by a low-order discretization will be particularly noticeable on scatterers whose cross section has a large dynamic range as a function of angle. We devised a large 2-D scatterer called the bat in order to demonstrate this effect. We observed that where the cross section is high, solutions computed using low-order and high-order basis functions were about the same, whereas in the more interesting regions where the cross section is low, the high-order solution is accurate while the low-order solution has significant errors. Had we used a low-order surface representation the result would likely have been worse still. The bat also demonstrated the practical utility of high-order methods for estimating the accuracy of a computed solution.

ACKNOWLEDGMENT

The authors are grateful to Prof. V. Rokhlin for many stimulating discussions regarding use of high-order methods in scattering calculations.

REFERENCES

[1] L. Hamilton, M. Stalzer, R. S. Turley, J. Visher, and S. Wandzura, "FastScat: An object-oriented program for fast scattering computation," *Sci. Programming*, vol. 2, no. 4, pp. 171–178, 1993.

[2] L. R. Hamilton, J. J. Ottusch, M. A. Stalzer, R. S. Turley, J. L. Visher, and S. M. Wandzura, "Accuracy estimation and high-order methods," in *11th Ann. Review of Progress in Applied Computational Electromagnetics*. Monterey, CA: Applied Computational Electromagnetics Society, vol. II, pp. 1177–1184, Mar. 1995.

[3] R. F. Harrington, *Field Computation by Moment Methods*. New York: Macmillan, 1968.

[4] S. M. Wandzura, "High-order regulation of singular kernels," in *Progress in Electromagnetics Research Symp.*, Univ. Washington, Seattle, WA, July 1995, p. 131.

[5] ——, "Electric current basis functions for curved surfaces," *Electromagnetics*, vol. 12, pp. 77–91, 1992.

[6] L. Hamilton, V. Rokhlin, M. Stalzer, R. S. Turley, J. Visher, and S. M. Wandzura, "The importance of accurate surface models in RCS computations," in *IEEE Antennas Propagation Soc. Symp. Dig.*, Ann Arbor, MI, vol. 3, June 1993, pp. 1136–1139.

[7] S. M. Wandzura, "Accuracy in computation of matrix elements of singular kernels," in *11th Ann. Review of Progress in Applied Computational Electromagnetics*. Monterey, CA: Applied Computational Electromagnetics Society, vol. II, pp. 1170–1176, Mar. 1995.

[8] ——, "High-order discretization of integral equations with singular kernels," in *IEEE Antennas Propagation Soc. Int. Symp. Dig.*, Newport Beach, CA, vol. 1, pp. 792–795, June 1995.

[9] J.-H. Ma, V. Rokhlin, and S. M. Wandzura, "Generalized Gaussian quadrature rules for systems of arbitrary functions," *SIAM J. Numerical Anal.*, vol. 33, pp. 971–996, June 1996.
[10] R. Coifman, V. Rokhlin, and S. M. Wandzura, "The fast multipole method: A pedestrian prescription," *IEEE Antennas Propagation Soc. Mag.*, vol. 35, pp. 7–12, June 1993.

Lisa R. Hamilton received the B.S. degree in engineering from the California State University, Northridge, in 1989.

She began her career at Hughes in 1989. Her early work included the simulation of automotive and missile control systems, and the analysis and design of infrared sensing and image processing systems. As a member of the Computational Physics Department at HRL Laboratories, she was involved for several years in the implementation of numerical methods for the calculation of electromagnetic scattering and radiation. She is currently an Advanced Project Engineer with Delphi Automotive Systems.

John J. Ottusch was born in Landstuhl, Germany, in 1955. He received the S.B. degree in physics in 1977 from the Massachusetts Institute of Technology, Cambridge, and the Ph.D. degree in physics in 1985 from the University of California, Berkeley, where he was a National Science Foundation fellow. His thesis research involved heterodyne spectroscopy of the sun in the infrared.

Since obtaining his graduate degree, he has been a member of the technical staff at Hughes Research Laboratories (now HRL Laboratories). From 1985 to 1994 his research was primarily devoted to experimental investigations of nonlinear optics, including stimulated Raman and Brillouin scattering and optical phase conjugation. Since 1994 he has been working on developing fast high-order algorithms and software for electromagnetic modeling.

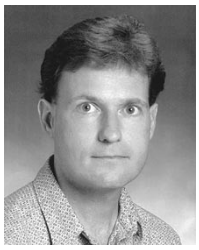

Mark A. Stalzer received the B.S. degree in physics and computer science from the California State University at Northridge and the M.S. and Ph.D. degrees in computer science from the University of Southern California.

He is a Senior Research Scientist in the Computational Physics Department of HRL Laboratories. His research interests include computational electromagnetics, algorithm design, and parallel processing.

Dr. Stalzer is a member of the ACM and Sigma Xi.

R. Steven Turley (SM'91) received the B.S. degree in physics (summa cum laude) from Brigham Young University, Provo, UT, in 1978 and the Ph.D. degree from Massachusetts Institute of Technology, Cambridge, in 1984.

In 1979 he joined Hughes Research Laboratories as a Member of the Technical Staff. He left Hughes in 1995 as a Senior Research Staff Scientist to join the faculty at Brigham Young University where he is currently an Associate Professor of Physics and Astronomy. His current areas of research interest include computational electromagnetics, XUV optics, and XUV sources.

Dr. Turley is a member of the American Physical Society, Sigma Xi, and the American Association of Physics Teachers.

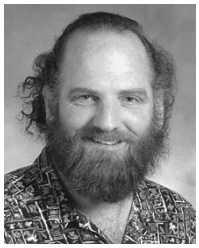

John L. Visher received the B.A. degree in physics from the University of California, Santa Cruz, in 1979 and the M.A. degree in physics from Columbia University, New York, NY, in 1981.

In 1985 he joined the Hughes Reserach Laboratories. His responsibilities were in the area of HEMT and HBT testing and design. He has also designed control software for focused ion beam systems, molecular beam epitaxy chambers, and assorted other machines used for the fabrication of electronic devices. His research interests are in the area of computational electromagnetics and he has recently written a high-order integral equation code to compute the interaction of electromagnetic fields with conducting surfaces and dielectric volumes.

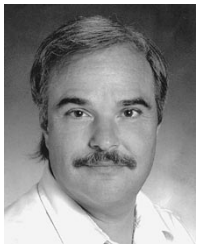

Stephen M. Wandzura received the B.S. degree in music from the University of California, Los Angeles, in 1971 and the Ph.D. degree in physics from Princeton University, Princeton, NJ, in 1977.

He is a Principal Research Scientist, Communications and Photonics Laboratory, HRL Laboratories. His research has been in diverse areas of scattering and propagation. His thesis research studied spin-dependent deep inelastic lepton-hadron scattering. As a National Research Fellow with the NOAA, he studied scattering of light by atmospheric turbulence and the occurrence of mountain lee waves. At HRL, he has worked on classical and quantum optics, especially the theoretical and numerical study of stimulated scattering. Since 1989, he has be studying numerical solution of scattering and radiation problems. He has published articles in *Physical Review*, *Physical Review Letters*, *Physics Letters*, *Optics Letters*, *Nuclear Physics*, *JOSA*, and other journals.